ELSEVIER

MHD oscillations in solar and stellar coronae: Current results and perspectives

Valery M. Nakariakov *

Physics Department, University of Warwick, Coventry CV4 7AL, UK

Abstract

Wave and oscillatory activity is observed with modern imaging and spectral instruments in the visible light, EUV, X-ray and radio bands in all parts of the solar corona. Magnetohydrodynamic (MHD) wave theory gives satisfactory interpretation of these phenomena in terms of MHD modes of coronal structures. The paper reviews the current trends in the observational study of coronal oscillations, recent development of theoretical modelling of MHD wave interaction with plasma structures, and implementation of the theoretical results for the mode identification. Also the use of MHD waves for remote diagnostics of coronal plasmas is discussed. In particular, the applicability of this method to the estimation of the coronal magnetic field is demonstrated.
© 2007 COSPAR. Published by Elsevier Ltd. All rights reserved.

1. Introduction

Wave and oscillatory processes in the solar and stellar coronae have been attracting researcher's attention for several decades. Traditionally, the interest is motivated by the possible role the waves playing in heating of the coronae and in the acceleration of solar and stellar winds, via the transfer and deposition of energy and mechanical momentum. Also, as waves and oscillations are associated with various dynamical phenomena in coronal plasmas, their study is fundamental for plasma astrophysics in general. With increased spatial and time resolution and sensitivity of modern observational instruments, it became possible to observe directly wave and oscillatory processes in solar coronal plasma structures. The progress recently reached in observational detection and theoretical modelling of solar coronal waves and oscillations provided the foundation for the development of *MHD coronal seismology*, the novel method for remote diagnostics of astrophysical plasmas. MHD seismology of the solar corona was theoretically suggested by Uchida (1970) for the global diagnostics of the corona, and by Roberts et al. (1984) for the diagnostics of coronal structures. However, practical implementation of this method became possible only in late 1990s, with the launch of the Solar and Heliospheric Observatory (SOHO) and the Transition Region and Coronal Explorer (TRACE) missions. Instruments onboard these spacecraft provided the necessary spatial, temporal and spectral resolution for confident detection and identification of various MHD modes of coronal structures. The success of coronal seismology in application to the solar corona motivated the interest to the implementation of this technique to the diagnostics of stellar coronae. These days, coronal seismology is a rapidly developing branch of modern astrophysics.

The characteristic periods of observed coronal oscillations are in the range from a second to several min. The typical spatial scales of the oscillations are 10^8–10^{10} Mm, and are comparable with the transverse and longitudinal characteristic spatial scales of solar coronal structures, e.g. the width and length of a typical coronal loop, respectively. The characteristic times are much longer and the spatial scales are much larger than the characteristic

* Tel.: +44 2476 522235.
  E-mail address: V.Nakariakov@warwick.ac.uk
  URL: http://www.warwick.ac.uk/go/space/

plasma physics times and scales, such as the proton gyration time, plasma oscillation period, gyroradii and Debye length, respectively. Moreover, the characteristic times of the oscillations are comparable with the expected transverse and longitudinal transit times of MHD waves in coronal structures. All above justifies the use of MHD theory for the description of wave and oscillatory processes observed in the corona.

The theoretical cornerstone of the coronal wave study, created by Zaitsev and Stepanov (1975) and by Roberts with co-authors (see, e.g. Roberts et al., 1984) is based upon the straight magnetic slab and cylinder models. The simple 1D inhomogeneity of the plasma allows to reduce the mathematical problem to a second order ordinary differential equation. Those models provide us with the classification of various MHD modes which can exist in coronal structures and reveal their dispersion properties. The majority of the theoretically predicted modes has been identified in the solar corona. The observational evidence of the wave and oscillations is abundant and it is impossible to cover all aspects of this research field in one paper. Comprehensive recent reviews of various issues of this topic can be found in e.g. Roberts (2000), Aschwanden (2004), Nakariakov and Verwichte (2005).

In stellar coronae, oscillatory processes are usually associated with quasi-periodic pulsations in flares. For example, Mathioudakis et al. (2003) observed 5 min white light intensity oscillations in a flare on the RS CV binary II Peg. The first detection of quasi-periodic pulsations in the X-ray emission generated by stellar coronal flares was recently reported by Mitra-Kraev et al. (2005). An oscillation with the period of 750 s was found in the soft X-ray flaring light curve on AT Mic, observed with XMM-Newton. The oscillation was quickly decaying with the decay time of about 2000 s. Also, oscillations in stellar flares are often detected as quasi-periodic low-frequency modulation of microwave emission. For example, Zaitsev et al. (2004) found the periodicities in the range 0.5–5 s in a flare on AD Leo.

Usually, MHD oscillations of coronal loops have an energy that is low in comparison with, e.g., flaring releases. Even in the solar corona, which is well-open to direct observational studies, the discoveries of MHD waves and oscillations were made on the very threshold of the available resolution. Obviously, the direct detection of loop oscillations in the coronae of other stars is impossible. However, quasi-periodic pulsations of flaring energy releases can also be associated with MHD oscillations. In particular, the typical periods of solar radio pulsations are often in the same range as the directly observed coronal MHD oscillations (Aschwanden, 1987, Nakariakov and Verwichte, 2005). Thus, the search for and identification of signatures of MHD oscillations in flares, together with the theoretical investigation of mechanisms for the modulation or triggering of flaring energy releases by MHD oscillations, is an important topic for the further progress of coronal wave studies. In particular, the development in

this direction opens up very interesting perspectives for the MHD diagnostics of stellar coronae.

Here, we restrict our attention to large scale oscillations of coronal structures, in particular coronal loops, discussing their properties, resonant periods, mechanisms for the emission modulation, diagnostic implementation and open questions connected with the development of solar and stellar coronal wave studies.

2. MHD modes of plasma structures

In ideal MHD, there are three basic MHD waves: an incompressible Alfvén wave, and fast and slow magnetoacoustic waves which are both essentially compressible. Properties of MHD waves strongly depend upon the angle between the wave vector and the magnetic field, consequently, MHD waves are highly affected by the non-uniformity of physical parameters in the plasma. Structuring of the coronal plasma modifies those waves and brings such interesting features of MHD wave dynamics as phase mixing and resonant absorption. Cylindrical and other quasi one- and two-dimensional structures (with the characteristic spatial scale in one dimension being much larger than in other dimensions) can guide magnetoacoustic waves. There is a number of various possible MHD modes in plasma waveguides (e.g. Roberts, 2000). This makes the theory of MHD wave modes of plasma structures the key ingredient of the coronal wave study. Also, the theory provides the necessary classification of wave and oscillatory phenomena in coronal plasmas.

The standard model for the study of linear MHD modes of coronal structures is a plasma cylinder. The equilibrium MHD plasma parameters: density, magnetic field, gas pressure experience a jump at the cylinder boundary ($r = 0$) which is considered to be discontinuous. In the internal and external media, the sound speeds are C_{s0} and C_{se}, and the Alfvén speeds are C_{A0} and C_{Ae}, respectively. For slow magnetoacoustic waves, it is convenient to introduce the tube speeds C_{T0} and C_{Te}, where $C_{T0,e} = C_{s0,e}C_{A0,e}/\sqrt{C_{s0,e}^2 + C_{A0,e}^2}$. Relations between those characteristic speeds determine properties of MHD modes guided by the tube. The total pressure is equal at both sides of the boundary. The formalism for the determination of MHD modes of this structure and for the derivation of their dispersion relations was developed by Zaitsev and Stepanov (1975) and by Edwin and Roberts (1983).

The longitudinal wave number k_z (along the cylinder axis) and the azimuthal wave number m, and the frequency ω are connected with each other by the dispersion relation

$$\rho_e(\omega^2 - k_z^2 C_{Ae}^2)m_0\frac{I'_m(m_0a)}{I_m(m_0a)} + \rho_0(k_z^2 C_{A0}^2 - \omega^2)m_e\frac{K'_m(m_ea)}{K_m(m_ea)} = 0,$$

(1)

where $I_m(x)$ and $K_m(x)$ are modified Bessel functions of order m, and the prime denotes the derivative with respect to argument x. Functions m_0 and m_e which may be considered

as radial wave numbers of the perturbations inside and outside the cylinder, respectively, are defined through

$$m_i^2 = \frac{(k_z^2 C_{\mathrm{si}}^2 - \omega^2)(k_z^2 C_{\mathrm{Ai}}^2 - \omega^2)}{(C_{\mathrm{si}}^2 + C_{\mathrm{Ai}}^2)(k_z^2 C_{\mathrm{Ti}}^2 - \omega^2)}, \tag{2}$$

where $i = 0$, e, the indices stand for the internal and external media, respectively. For modes that are confined to the tube (evanescent outside, in $r > a$), the condition $m_{\mathrm{e}} > 0$ has to be fulfilled. The choice of the modified Bessel functions $K_m(x)$ for the external solution is connected with the demand of the exponential evanescence of the solution outside the loop (*trapped modes*). Phase speeds of the trapped modes form two bands, from C_{T0} to C_{s0}, and from C_{A0} to C_{Ae}, corresponding to the slow and fast modes, respectively. The slow modes are essentially longitudinal and can be considered as modified acoustic waves.

The integer m, the azimuthal mode number, determines the azimuthal modal structure: waves with $m = 0$ are *sausage* (or radial, fast magnetoacoustic, peristaltic) modes, waves with $m = 1$ are *kink* modes, waves with $m > 2$ are referred to as *flute* or ballooning modes. For $m_0^2 < 0$, the internal radial structure of the modes is described by the Bessel functions $J_m(x)$, and the radial dependence of the oscillation inside the cylinder is quasi-periodic. The radial number l is connected with the number of oscillation maxima in the cylinder in the radial direction. There is an infinite number of modes with a given azimuthal number m, corresponding to different radial numbers l. The modes with higher radial numbers l have higher phase speeds along the loop and exist for higher values of the longitudinal wave number k_z. For standing modes, the boundary conditions in the longitudinal direction lead to the quantification of the longitudinal wave number k_z, introducing a longitudinal wave number n which is an integer corresponding to the number of maxima of the transverse velocity perturbations along the loop.

Thus, the dispersion relation (1) allows us to determine the frequency of a trapped magnetoacoustic mode if the integer mode numbers, the longitudinal number n, the radial number l and the azimuthal number m are given. The existence and properties of the modes are determined by the equilibrium physical quantities. A dispersion plot, typical for a flaring coronal loop, is shown in Fig. 1. The ratio of the sound speed to the Alfvén speed is possibly higher than in reality. The figure shows that trapped magnetoacoustic modes have phase speeds in two bands, the fast one, between the Alfvén speeds inside and outside the loop, and the slow one, between the internal tube and sound speeds. Modes in these bands correspond to the modified fast and slow waves, respectively.

Four main MHD modes of a coronal loop are the sausage, kink, longitudinal and torsional modes. The longest period modes, with the wavelength equal to double the loop length, are called global (fundamental, principal).

The period P_{saus} of the global sausage mode ($m = 0$, $n = 1$, $l = 0$) of a coronal loop of the length L is
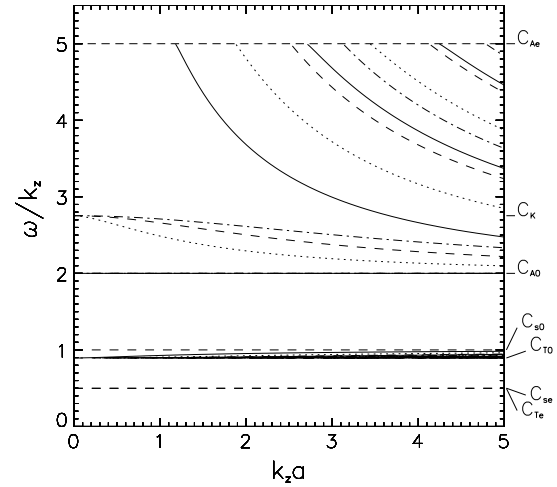

Fig. 1. A typical dispersion diagram showing the real phase speed solutions of dispersion relation (1) for MHD waves in a magnetic cylinder as a function of the normalised longitudinal wave number $k_z a$. The phase speed is measured in units of the internal sound speed. The characteristic speeds in the internal and external media are shown relative to the internal sound speed: $C_{\mathrm{A0}} = 2$ C_{s0}, $C_{\mathrm{Ae}} = 5$ C_{s0} and $C_{\mathrm{se}} = 0.5$ C_{s0}. The solid, dotted, dashed and dot-dashed curves correspond to solutions with the azimuthal wave number m equal to 0, 1, 2 and 3, respectively. The torsional Alfvén wave mode solution is shown as a solid line at $\omega/k_z = C_{\mathrm{A0}}$ (from Nakariakov and Verwichte, 2005).

$$P_{\mathrm{saus}} = 2L/C_{\mathrm{p}}, \tag{3}$$

where C_{p} is the phase speed of the sausage mode corresponding to the wave number $k_z = \pi/L$, $C_{\mathrm{A0}} < C_{\mathrm{p}} < C_{\mathrm{Ae}}$. The sausage mode has a long wavelength cutoff given by the critical wave number

$$k_{zc} = \frac{j_0}{a} \left[\frac{(C_{\mathrm{s0}}^2 + C_{\mathrm{A0}}^2)(C_{\mathrm{Ae}}^2 - C_{\mathrm{T0}}^2)}{(C_{\mathrm{Ae}}^2 - C_{\mathrm{A0}}^2)(C_{\mathrm{Ae}}^2 - C_{\mathrm{s0}}^2)} \right]^{1/2}, \tag{4}$$

where $j_0 \approx 2.40$ is the first zero of the Bessel function $J_0(x)$. Trapped sausage modes can exist only if their longitudinal wave numbers are greater than the cutoff value. For $k_z \to k_{zc}$, C_{p} tends to C_{Ae} from below, and for $k_z \to \infty$, C_{p} tends to C_{A0} from above. Also, the length of the loop L should be smaller than π/k_{zc} to satisfy the condition $k > k_{zc}$.

The period of the global kink mode ($m = 1$, $n = 1$, $l = 0$) is

$$P_{\mathrm{kink}} = \frac{2L}{C_{\mathrm{k}}}, \tag{5}$$

where the kink speed

$$C_{\mathrm{k}} \equiv \left(\frac{2}{1 + \rho_{\mathrm{e}}/\rho_0} \right)^{1/2} C_{\mathrm{A0}}. \tag{6}$$

Normally, the kink speed is closer to the Alfvén speed inside the loop. As any transverse mode, the kink mode can have either vertical or transverse polarisation, or be their combination. In the cylinder model, both these polarisations have the same phase speed, so the same oscillation period. However, it is still not clear whether this remains

the same in the case of more realistic, curved loops. The preliminary studies (Van Doorsselaere et al., 2004) showed that the phase speeds of vertically and transversely polarised kink modes of curved loops are quite close to each other, which justifies the use of the cylinder model.

The period of the global longitudinal mode is given by the expression

$$P_{\mathrm{long}} = 2L/C_{\mathrm{T0}}. \tag{7}$$

In the low-β plasma typical for coronal conditions, the internal tube speed C_{T0} is very close to the internal sound speed C_{s0}, hence the period P_{long} is practically determined by the temperature in the loop and should evolve together with it.

The theory introduced above does not take into account another MHD mode, the torsional one. Torsional waves are twistings of the tube, propagating at the local Alfvén speed. In a coronal loop, the resonant period of the global torsional mode is

$$P_{\mathrm{tors}} = 2L/C_{\mathrm{A0}}. \tag{8}$$

The above theory misses several potentially important physical effects, such as the loop curvature, possible smoothness of the loop density and magnetic field profile and twisting of the magnetic field. In addition, in the case of cooler loops, when the scale height is sufficiently small and can be comparable with wave length, the stratification should be taken into account. There have been several studies of the potential importance of these effects, see e.g. Nakariakov and Roberts (1995); Zhugzhda and Nakariakov (1999); Mendoza-Briceño et al. (2004); Van Doorsselaere et al. (2004); Verwichte et al. (2006).

3. Mechanisms for the emission modulation by MHD modes

3.1. MHD waves in emitting spectra

Periodic variation of MHD properties of a plasma can modulate the EM emission by several fashions. First of all, it is the modulation of thermal emission associated with certain spectral lines. The change in the plasma temperature (e.g., by non-isothermal magnetoacoustic waves) can be detected as periodic broadening of the corresponding spectral lines. Periodic alternate bulk flows (motions) of the plasma along the line-of-sight (LOS) cause the periodic Doppler shifts of the line. This trivial picture can be seriously complicated by the resolution of the instrument.

Different MHD modes have different spectral observational signatures. First of all, the intensity of the spectral line can be modulated by the density perturbations induced by the oscillations. Also, the intensity can be modulated by the variation of the LOS (see discussion in Section 3.2) and/or by the motion of the oscillating structure with respect to the FOV, e.g. periodically coming to and leaving the spectrometer observational slit.

Also, a mode can be detected as some variation of the spectrum if it induces bulk plasma flows with a sufficiently large LOS component. The Doppler effect leads to the shift of the emission line wavelength, $\Delta\lambda = \lambda V/c$, where λ is the original wavelength, and V/c is the ratio of the LOS component of the flow speed and the speed of light. For example, the LOS should have a sufficiently small angle to the plane of kink oscillations, to allow for their detection. The sausage mode can be observed with any orientation of the LOS. This mode can be seen as periodic non-thermal broadening of the emission line, as it induces LOS-aligned flows in both inward and outward directions simultaneously. The torsional mode has the same observational signature if the spectrometer cannot resolve the loop width, as, e.g. the presently available spectrometers. Forward modelling of observational signatures of torsional modes for various radial structures of the oscillation can be found in Williams (2004).

The longitudinal mode, which produces field-aligned flows, can be seen as the periodic Doppler shift of an emission line in the case when the loop plane has a sufficiently small angle to the LOS.

3.2. Modulation of thermal emission by compressible waves

In the EUV and soft X-ray band, the emission intensity $\mathcal{I}$, associated usually with heavy ions, is modulated by the density perturbations $\tilde{\rho}$ in the compressible (fast and slow magnetoacoustic) waves as

$$\mathcal{I} \propto (\rho_0 + \tilde{\rho})^2 \approx \rho_0^2 + 2\rho_0\tilde{\rho}, \tag{9}$$

where ρ_0 is the background density, and it is assumed that $\rho_0 \gg \tilde{\rho}$. Thus, the weak perturbations of the density are observed to be two times stronger in the emission intensity amplitude.

An important issue is the LOS effect (Cooper et al., 2003). Even an incompressible perturbation can change the angle between the local axis of an emitting loop and the LOS, causing the change of the observed column depth. Hence, the intensity of the observed emission is modulated by the incompressible perturbation. In particular, almost incompressible kink modes can cause such modulation of the emission intensity.

3.3. Modulation of the electron precipitation rate

Strong modulation depth of flaring white light and hard X-ray emission can be produced by periodic variation of the non-thermal electron precipitation rate by MHD oscillations (Zaitsev and Stepanov, 1982). Diverging flaring loops are magnetic traps for the electrons, accelerated by flares. The electrons with sufficiently large pitch angle α bounce between the magnetic mirrors created by the converging magnetic flux tube at the loop legs. The range of the pitch angles of the trapped electrons is determined by the ratio of the magnetic fields at the loop top, B_{top}, and near the loop footpoint, B_{fp},

$$\cot^2 \alpha < \frac{B_{\text{fp}} - B_{\text{top}}}{B_{\text{top}}}. \tag{10}$$

Magnetoacoustic oscillations can periodically change the strength of the magnetic field at the loop top, varying the mirror ratio given by Eq. (10). Hence, the critical pitch angle will be periodically modulated, leading to the periodic escape of the particles from the trap downward towards the loop footpoints. Reaching the lower layers of the atmosphere, the electrons interact with the dense plasma and cause hard X-ray and white light emission. This effect can be associated with the sausage mode and, if the plasma β is sufficiently large, with the longitudinal mode.

3.4. Modulation of gyrosynchrotron emission by a loop MHD-oscillations

Another important issue is the modulation of observed emission by the variation of the plasma parameters perturbed by MHD waves. In particular, broadband microwave bursts are generated by the gyrosynchrotron emission mechanism which is very sensitive to the magnetic field in the radio source. The intensity of optically thin gyrosynchrotron emission at a frequency f is connected with the absolute value of the magnetic field, B and the angle between the magnetic field and the LOS, θ, by Dulk and Marsh's approximated formula (Dulk and Marsh, 1982)

$$
\begin{aligned}
I_{\text{f}} \approx \frac{BN}{2\pi} &\times 3.3 \times 10^{-24} \\
&\times 10^{-0.52\delta} (\sin\theta)^{-0.43 + 0.65\delta} \left(\frac{f}{f_{\text{B}}}\right)^{1.22 - 0.90\delta},
\end{aligned} \tag{11}
$$

where N is the concentration of the nonthermal electrons with the energies higher than 10 keV, measured in cm^{-3}, f_{B} is the gyrofrequency and δ is the power law spectral index of the electrons, the magnetic field is measured in G. The quasi-periodic variations of the value B and direction of the magnetic field θ can be associated with the kink, torsional and sausage modes.

Also, in the lower frequency part of the gyrosynchrotron spectrum, the modulation of the microwave emission can be produced by slow magnetoacoustic waves (Nakariakov and Melnikov, 2006). The modulation mechanism is based upon perturbation of the Razin suppression efficiency of optically thin gyrosynchrotron emission. The suppression of radiation from an electron happens in a medium in which the index of refraction is less than unity. This effect is controlled by the ratio of the plasma frequency and gyrofrequency. Variations of the plasma density by an acoustic wave change the plasma frequency and hence Razin suppression. Forward modelling of microwave signatures of standing longitudinal waves showed that the observed depth of the modulation produced by the wave can be up to an order of magnitude higher than the original amplitude of the oscillation.

3.5. Periodic triggering of flares by MHD oscillations

According to expressions (3), (5), (7), (8), the periods of MHD oscillations are determined, in particular, by the geometric size of the oscillating plasma structure. However, often, the periods given by formulae (3), (5), (7), (8) with the use of the observed geometrical sizes of oscillating structures are quite different from the observed periods.

Recently, Nakariakov et al. (2006) developed a model which can explain the coupling of loop oscillations with quasi-periodic pulsations of flaring energy releases. It was suggested that periods of the pulsations observed in a flaring loop or at its footpoints are produced by MHD oscillations in another loop situated nearby, which is not necessarily magnetically linked with the flaring one. In the model, the MHD oscillations are not considered to be responsible for the flaring energy release itself, but play the role of periodic triggering. The period of the oscillations is determined by the size of the oscillating loop. The linkage of the oscillation with the flare site is carried out by the external, evanescent or leaky, part of the oscillation. From the point of view of the flaring (or, rather, pre-flare) site, this part of the oscillation is a perpendicular fast magnetoacoustic wave with the period prescribed by the oscillation. Approaching a magnetic non-uniformity at the flare site, e.g. a magnetic null point, the amplitude of the wave, as well as the density of the periodically varying electric current produced by the wave, increases to very large values (see also the detailed investigation of this effect by McLaughlin and Hood, 2004). The variations of the current density can induce current-driven plasma micro-instabilities and thus anomalous resistivity (see Büchner and Elkina, 2005 for a review). This can periodically trigger magnetic reconnection, and hence acceleration of charged particles, producing quasi-periodic pulsations of X-ray, optical and radio emission at the arcade footpoints.

Recently, Foullon et al. (2005) analysed 10 min quasi-periodic pulsations in two remotely situated flares observed with the Reuven Ramaty High Energy Spectroscopic Imager (RHESSI) and other instruments. The geometrical sizes of the flaring active regions could not explain the long periods of the pulsations. On the other hand, the observed dynamics of these two flaring sites showed a clear similarity. It was suggested that, the pulsations were likely to have a common source and be caused by kink mode oscillations in an external large loop linking the flaring sites. Indeed, such a loop, although very faint, was found in the EUV band.

4. Direct observations of solar coronal loop oscillations

In the following, I present observations of various MHD modes of solar coronal structures, performed with the spatial and temporal resolution sufficiently good to identify the modes.

4.1. Kink oscillations

Possibly, the first observation of transverse oscillations of coronal loops, associated with the kink fast magnetoacoustic mode was made by Koutchmy et al. (1983). The analysis of the time variation of the coronal "green" line, associated with the emission of the Fe XIV ion, revealed Doppler velocity oscillations with periods near 43, 80 and 300 s. There were no intensity variations observed.

The first imaging observation of the kink mode became possible with the use of the EUV imager TRACE. Aschwanden et al. (1999) and Nakariakov et al. (1999) studied decaying oscillating transverse displacements of EUV coronal loops observed in 171and 195 Å. Oscillations of different loops were not in phase. The highest displacement amplitude, of a few Mm, was seen near loop apices. The characteristic periods of the observed oscillations were of several minutes for the observational cadence time of about 70 s. The oscillations were quickly decaying, in just a few periods. Since the discovery, this phenomenon has attracted great attention from both observers and theoreticians (see e.g. Nakariakov and Verwichte, 2005 and references therein). It is now commonly accepted that the transverse oscillation is the global kink (or $m = 1$) fast magnetoacoustic mode. According to Aschwanden et al. (2002) the typical observable parameters of the oscillations are: the period of 5.4 ± 2.3 min, the decay time of 9.7 ± 6.4 min and the displacement amplitude of 0.1–2.8 Mm. The oscillations are usually seen for about four periods only.

Recently, the analysis of oscillations in an off-limb coronal arcade gave the evidence of the second spatial harmonics of this mode (Verwichte et al., 2004) with the period about 240 s, approximately a half of the observed global mode period, 400 s. The oscillations at the second harmonics were found in the loop legs with the use of the time–distance technique. This mode is not seen at the loop top, where the global mode has the highest displacement amplitude. This is consistent with the theoretically predicted structure of the second harmonics, which has a node at the loop top. The period of the second harmonics is not exactly equal to the half of the fundamental mode period, because of dispersion: the phase speed of the kink mode varies with the wave number.

The kink mode can also be associated with the Doppler-shift oscillations measured during solar flares in emission lines of S XV and Ca XIX with the Bragg Crystal Spectrometer (BCS) on Yohkoh (Mariska, 2006). Fig. 2 shows typical Doppler shift variations observed with BCS. However, for some of the flares, intensity fluctuations are also observed. These lag the Doppler-shift oscillations by 1/4 period, strongly suggesting that at least these oscillations are standing longitudinal mode waves (discussed in Section 4.3).

The direct linkage of the oscillation period with the Alfvén speed in the loop provides us with a tool for the estimation of the coronal magnetic field – a good example of MHD coronal seismology. The practical formula for the determination of the field is

$$B_0 = \sqrt{\mu_0 \rho_0} C_{A0} \approx \frac{\sqrt{2\mu_0}L}{P} \sqrt{\rho_0(1 + \rho_e/\rho_0)}, \qquad (12)$$

where L is the loop length, P is the measured period of the oscillations, and other notations are the same as in Section 2. For the first time this method was applied by Nakariakov and Ofman (2001), who determined the absolute value of the magnetic field in a loop as 13 ± 9 G. The large error bars are mainly connected with the uncertainty in the determination of the density inside the loop with TRACE. Estimations in approximately the same range were obtained by Verwichte et al. (2004) for nine off-limb loops.

4.2. Sausage oscillations

The sausage (or $m = 0$) fast magnetoacoustic mode is a symmetric perturbation of the loop cross-section, accompanied by the perturbation of the magnetic field and the plasma density which are in phase with each other.

The first identification of the sausage mode in the solar corona was made by Nakariakov et al. (2003) in the microwave band with the use of the Nobeyama radioheliograph (NoRH). The instrument has a very good time resolution (0.1 or 1 s) and quite a reasonable spatial resolution (11 in. at 17 GHz and 5 in. at 34 GHz). In particular, it allows the study of the gyrosynchrotron emission produced by flare-accelerated relativistic electrons guided by coronal loops. For a flare on the 12th of January, 2000, Nakariakov et al. (2003) found that the time profiles of the microwave emission at 17 and 34 GHz exhibit synchronous quasi-periodic variations of the intensity with the period of about 16 s in different parts of the corresponding flaring loop. The mean amplitude of the observed quasi-periodic pulsations reached 100 s.f.u. The length of the oscillating loop was estimated as $L = 25$ Mm and its width at half intensity at 34 GHz as about 6 Mm. These estimations were confirmed by Yohkoh/SXT images taken on the late phase of the flare. The distribution of the spectral density in the interval 14–17 s along the loop showed the peak of oscillation amplitude near the loop apex and depression at the loop legs, consistent with the structure theoretically predicted for a global mode.

Further study of this event in microwave and hard X-ray bands was performed by Melnikov et al. (2005). The main attention was paid to the second peak detected at about 9 s, which was found to be relatively stronger at the loop legs (near the footpoints). The pulsations at both loop legs are well correlated with the period $P_2 = 8$–11 s, while the correlation between the pulsations at the legs and at the apex is not so pronounced. Also, a definite phase shift, about a quarter of the period, 2.2 s, between pulsations in the northern leg and top part of the loop was found. This second mode was shown to be consistent with the third harmonics of the sausage mode, however the alternative interpretation as the second and the third harmonics of the kink mode, and the second harmonics of the ballooning mode are also possible.
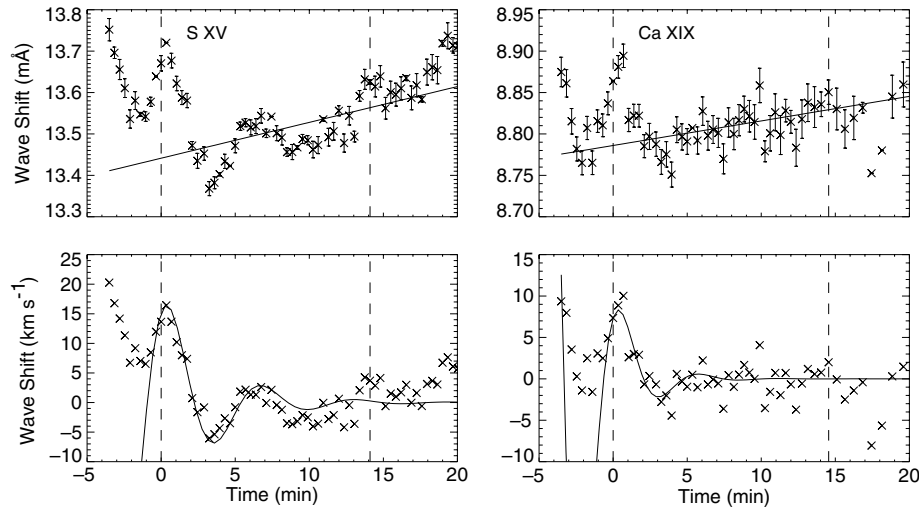
Fig. 2. Averaged BCS Doppler-shift data and decaying sine wave fits for the S XV and Ca XIX observations for the 1991 October 21 flare (Mariska, 2006).

Perhaps, the 6-s oscillations in the flare observed by NoRH and studied by Asai et al. (2001) (see Fig. 3) and Grechnev et al. (2003) are also associated with the sausage mode. More work is to be done to prove or refute this interpretation.

As it was pointed out by Nakariakov et al. (2003), the sausage mode provides us with an interesting opportunity for the estimation of the magnetic field value outside the oscillating loop. If its wave number is about the cut-off, the period of the mode is connected with the external Alfvén speed (see Eq. (3)). The practical formula for the determination of the field is

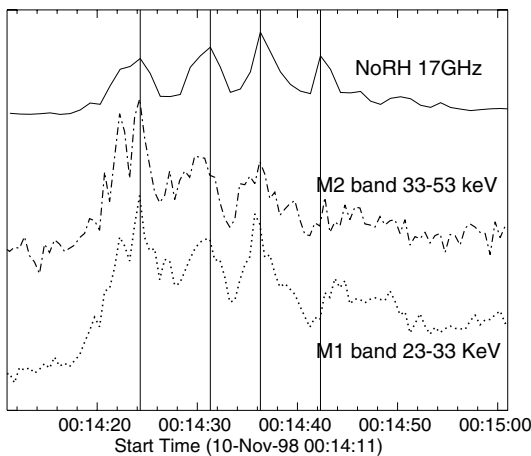$$B_{\mathrm{e}} = \frac{2L\sqrt{\mu_0 \rho_{\mathrm{e}}}}{P}, \tag{13}$$

Fig. 3. Light curves of flaring emission (scaled arbitrarily). From top to bottom: microwave brightness temperature observed at 17 GHz by NoRH (solid line) and hard X-ray count rate measured in the M2 band (33–53 keV; dash-dotted line) and M1 band (23–33 keV; dotted line) of Yohkoh/HXT. The vertical lines show the peak times of the microwave emission (from Asai et al., 2001).

where L is the loop length, P is the measured period of the oscillations and ρ_{e} is the external equilibrium density. The latter quantity may be difficult to be determined observationally. However, the observational determined density contrast ratio across the loop and the use of the total pressure balance condition provide the required estimation.

4.3. Longitudinal oscillations

There are two kinds of longitudinal compressible oscillations in the corona: propagating waves observed in polar plumes and near the loop footpoints, and standing waves sometimes referred to as "SUMER" oscillations. The propagating longitudinal, or slow magnetoacoustic waves in the corona are out of scope of this review. Detailed discussion of this phenomenon can be found in Nakariakov and Verwichte (2005).

Long period oscillations with the periods of several min, associated with longitudinal waves were found as periodic Doppler shift of the Fe XIX and Fe XXI emission lines observed with SOHO/SUMER in hot (about 6 MK) coronal loops (e.g. Wang et al., 2002). Later on, oscillations in the emission intensity, the necessary ingredient of compressible waves, were also found (Wang et al., 2003). Moreover, the measured phase shift between the velocity and the intensity oscillations was found to be about a quarter of the oscillation period, exactly as the theoretical prediction for a standing acoustic wave. The phenomenon of longitudinal oscillations seems to be quite widespread in the corona. For example, in April–May 2002, during an observing time interval of 18.4 days, 19 events were observed (Wang et al., 2003). Often, the oscillations are recurrent, i.e. they recur 2–3 times within about 2 h at the same place and manifest similar oscillation features such as identical periods and initial Doppler shifts of the same sign.

The typical periods of the longitudinal oscillations are in the range of 7–31 min. Similarly to kink oscillations,

longitudinal oscillations are quickly decaying, with the ratio of the period to the decay time of about unity. The average number of observed periods is 2.3 ± 0.7. The decay time scales approximately linearly with the oscillation period. The maximum velocity amplitudes are 75 ± 53 km/s, which is quite large in comparison with the sound speed in the oscillating loop, about 380 km/s.

The longitudinal oscillations have been interpreted by Ofman and Wang (2002) as a standing slow magnetoacoustic wave. A 1D model incorporating nonlinear effects and finite thermal conduction was developed. In particular, it was demonstrated that the oscillation period was determined by expression (7). Now, this interpretation is commonly accepted and it is believed that the observed mode is the fundamental one. According to MHD simulations of a coronal loop's response to a localised impulsive energy deposition (Nakariakov et al., 2004), the second harmonics of the longitudinal mode is also excited very effectively. The preferable excitation of the second harmonics can be explained as following: localised deposition of energy near the apex of the loop leads to development of two heat fronts going along the loop in the opposite directions towards the footpoints. Approaching the footpoints, the heat fronts cause evaporation of the plasma, upflows and upwardly propagating acoustic waves. This structure corresponds to the second harmonics. For the efficient excitation of the global mode, the upflow should be generated at only one of the footpoints. This can be produced, e.g., by a heat source localised near this footpoint. In this case, the opposite footpoint will be reached by heat front almost simultaneously with the acoustic wave generated at the first footpoint. The lack of imaging information does not allow us to distinguish between the fundamental longitudinal modes and its second harmonics in observations.

Possibly, the same phenomenon was observed by Sakurai et al. (2002) in the Doppler shift of the coronal green line Fe XIV (corresponding to the temperature of about 2 MK) with the Norikura coronograph. At localised regions, 2–3 and 5–16 min periodicities were detected. Some variations of the intensity were observed too, of about 1% of the background intensity. In one of the analysed cases the intensity oscillations were shifted with respect to the velocity oscillation by a quarter period. In addition, the velocity oscillations detected with Yohkoh/BCS by Mariska (2006, see the discussion in Section 4.1) can be of the acoustic nature too.

4.4. Torsional oscillations

In untwisted loops, torsional modes are incompressible and do not perturb the loop axis and boundaries, and hence these modes cannot be observed with coronal imagers. However, these modes can be detected with spectral instruments through the variation of the non-thermal broadening. The Doppler shift caused by torsional modes is different from the shift caused by longitudinal modes discussed in Section 4.3: in the torsional mode, the plasma moves in the direction perpendicular to the equilibrium magnetic field. Thus, the best observational conditions are when the oscillating loop is perpendicular to the LOS. Also, in the torsional mode, the twisting of a loop segment causes the perpendicular motions towards and outwards the LOS, simultaneously. In addition, the longitudinal mode is essentially compressible, while the torsional mode of an untwisted loop is incompressible. (See, however, Zhugzhda and Nakariakov, 1999, who demonstrated that in twisted tubes torsional modes are weakly compressible). In the same loop, for the same mode number, the period of a torsional mode is shorter than the period of the longitudinal mode, as the Alfvén speed is larger than the sound speed.

Zaqarashvili (2003) suggested that the global torsional oscillations may be observed as a periodical variation of the spectral line width along the loop. The amplitude of the broadening is maximum at the velocity antinodes and minimum at the nodes of the torsional oscillation. Observational evidence of the global torsional modes of coronal loops was found by Zaqarashvili (2003) in time series of Fe XIV coronal emission line spectra above an active region at the solar limb. The Doppler width temporal variations with the period of 6.1 ± 0.6 min were detected. The width fluctuations were enhanced in two 5.5 Mm long segments at heights of 66 and 88 Mm above the limb. The amplitude of variation was 0.125 Å at 88 Mm, while at lowest heights it reduces to 0.04 Å.

5. Conclusions

The last decade brought interesting and important advances in the theoretical and observational (both ground-based and spaceborne) studies of solar and stellar coronal MHD oscillations. In the solar corona, systematic observational investigation of various waves and oscillations became possible. Combined with the recent achievements in MHD wave theory, this provided the basis for the development and practical implementation of MHD diagnostics of the solar coronal plasma. This approach is believed to be promising for stellar coronae too. In the following, I discuss open questions and directions for future research in this field.

Kink oscillations of coronal loops are perhaps the most understood coronal oscillatory phenomenon. Nevertheless, there are still certain problems. First of all, we still do not understand the excitation mechanism and its selectivity. Most likely, the oscillations are excited by a flare-generated coronal blast wave, however it is not clear why some loops respond to the excitation while others do not. The decay mechanism has been subject to very intensive debates since the observational discovery of this mode. The options are resonant absorption, phase mixing with enhanced sheer viscosity; possibly leakage in the corona in multi-thread systems (see Nakariakov and Verwichte, 2005 and references therein for more detail discussion). The role of nonlinear effects (the displacement is greater than the loop width) is

not understood yet even theoretically. It is not clear whether the oscillations change the loop cross-section shape. Also, coupling of oscillations of neighbouring loops, and the question whether active regions oscillate as a whole, remain to be investigated.

There are many open questions connected with the sausage mode too. There have not been thorough studies of the excitation mechanisms. The strong modulation of the emission by this mode needs to be explained. The effects of the loop curvature and divergence on the oscillation period are not understood, but likely to play an important role in dispersion relation of this mode. Multi-wavelength imaging observations of the sausage mode, e.g. in microwave and in soft X-ray, would be very useful.

Observational evidence of the oscillations on the standing longitudinal mode is abundant. However, the selectivity of this mode excitation is not understood. Why is this mode seen predominantly in hot loops, where the mode damping because of thermal conduction is strongest? Observations of this mode with soft X-ray imagers in a loop perpendicular to the LOS and simultaneous lack of the velocity oscillations would strongly support its interpretation as a slow magnetoacoustic wave. As a predominantly acoustic wave, the longitudinal mode is strongly affected by thermodynamical properties of the medium, in particular by the heating function. Development of seismological techniques for the determination of the coronal heating function by longitudinal oscillations of coronal loops is an interesting theoretical challenge. Also, as flaring loops can have a sufficiently large β, longitudinal oscillations can allow for the estimation of the magnetic field in the loop by the difference between the tube speed (the measured phase speed of the oscillations, which depends upon the magnetic field) and the sound speed (which is determined by the temperature of the emitting plasma).

Torsional modes are still to be identified in observations with high spectral and spatial resolution. This makes forward modelling of observational signatures of these modes in various observational bands an important task. The theoretical development should include the investigation of the preferable excitation conditions, in particular, the determination of the probable transverse profile of torsional perturbations; linear and nonlinear mode coupling; and the effect of the equilibrium twist.

The correct identification of various MHD modes in solar and stellar coronae should be based upon the MHD wave theory. In particular, time evolution of various parameters of the oscillations can give us important information. For example, the oscillation period of a longitudinal oscillation should evolve with the temperature of the emitting plasma, which is an independent observable. Another important degree of freedom can be provided by multi-wavelength observations. For example, the modulation of microwave and hard X-ray emission by sausage modes should be accompanied by the modulation of the soft X-ray emission intensity, connected with the perturbation of plasma density by this mode.

All the above makes the study of coronal oscillations an interesting and important research area of modern astrophysics.

References

Asai, A., Shimojo, M., Isobe, H., et al. Periodic acceleration of electrons in the 1998 November 10 solar flare. Astrophys. J. 562, L103–L106, 2001.

Aschwanden, M.J. Physics of the Solar Corona. Springer Praxis Books, Berlin, 2004.

Aschwanden, M.J. Theory of radio pulsations in coronal loops. Sol. Phys. 111, 113–136, 1987.

Aschwanden, M.J., dePontieu, B., Schrijver, C.J., et al. Transverse Oscillations in coronal loops observed with TRACE II. Measurements of geometric and physical parameters. Sol. Phys. 206, 99–132, 2002.

Aschwanden, M.J., Fletcher, L., Schrijver, C.J., et al. Coronal loop oscillations observed with the transition region and coronal explorer. Astrophys. J. 520, 880–894, 1999.

Büchner, J., Elkina, N. Vlasov code simulation of anomalous resistivity. Space Sci. Rev. 121, 237–252, 2005.

Cooper, F.C., Nakariakov, V.M., Tsiklauri, D. Line-of-sight effects on observability of kink and sausage modes in coronal structures with imaging telescopes. Astron. Astrophys. 397, 765–770, 2003.

Dulk, G.A., Marsh, K.A. Simplified expressions for the gyrosynchrotron radiation from mildly relativistic, nonthermal and thermal electrons. Astrophys. J. 259, 350–358, 1982.

Edwin, P.M., Roberts, B. Wave propagation in a magnetic cylinder. Sol. Phys. 88, 179–191, 1983.

Foullon, C., Verwichte, E., Nakariakov, V.M., et al. X-ray quasi-periodic pulsations in solar flares as magnetohydrodynamic oscillations. Astron. Astrophys. 440, L59–L62, 2005.

Grechnev, V.V., White, S.M., Kundu, M.R. Quasi-periodic pulsations in a solar microwave burst. Astrophys. J. 588, 1163–1175, 2003.

Koutchmy, S., Zhugzhda, I.D., Locans, V. Short period coronal oscillations – observation and interpretation. Astron. Astrophys. 120, 185–191, 1983.

Mariska, J.T. Characteristics of solar flare Doppler-shift oscillations observed with the Bragg Crystal Spectrometer on Yohkoh. Astrophys. J. 639, 484–494, 2006.

Mathioudakis, M., Seiradakis, J.H., Williams, D.R., et al. White-light oscillations during a flare on II Peg. Astron. Astrophys. 403, 1101–1104, 2003.

McLaughlin, J.A., Hood, A.W. MHD wave propagation in the neighbourhood of a two-dimensional null point. Astron. Astrophys. 420, 1129–1140, 2004.

Melnikov, V.F., Reznikova, V.E., Shibasaki, K., et al. Spatially resolved microwave pulsations of a flare loop. Astron. Astrophys. 439, 727–736, 2005.

Mendoza-Briceño, C.A., Erdélyi, R., Sigalotti, L.D.G. The effects of stratification on oscillating coronal loops. Astrophys. J. 605, 493–502, 2004.

Mitra-Kraev, U., Harra, L.K., Williams, D.R., et al. The first observed stellar X-ray flare oscillation: constraints on the flare loop length and the magnetic field. Astron. Astrophys. 436, 1041–1047, 2005.

Nakariakov, V.M., Foullon, C., Verwichte, E., et al. Quasi-periodic modulation of solar and stellar flaring emission by magnetohydrodynamic oscillations in a nearby loop. Astron. Astrophys. 452, 343–346, 2006.

Nakariakov, V.M., Melnikov, V.F. Modulation of gyrosynchrotron emission in solar and stellar flares by slow magnetoacoustic oscillations. Astron. Astrophys. 446, 1151–1156, 2006.

Nakariakov, V.M., Melnikov, V.F., Reznikova, V.E. Global sausage modes of coronal loops. Astron. Astrophys. 412, L7–L10, 2003.

Nakariakov, V.M., Ofman, L. Determination of the coronal magnetic field by coronal loop oscillations. Astron. Astrophys. 372, L53–L56, 2001.

Nakariakov, V.M., Ofman, L., Deluca, E.E., et al. TRACE observation of damped coronal loop oscillations: implications for coronal heating. Science 285, 862–864, 1999.

Nakariakov, V.M., Roberts, B. On fast magnetosonic coronal pulsations. Sol. Phys. 159, 399–402, 1995.

Nakariakov, V.M., Tsiklauri, D., Kelly, A., et al. Acoustic oscillations in solar and stellar flaring loops. Astron. Astrophys. 414, L25–L28, 2004.

Nakariakov, V.M., Verwichte, E. Coronal waves and oscillations. Living Reviews in Solar Physics 2, 3, URL(05/07/2005):, 2005 http://www.livingreviews.org/lrsp-2005-3, 2004.

Ofman, L., Wang, T. Hot coronal loop oscillations observed by SUMER: slow magnetosonic wave damping by thermal conduction. Astrophys. J. 580, L85–L88, 2002.

Roberts, B. Waves and oscillations in the corona – (Invited review). Sol. Phys. 193, 139–152, 2000.

Roberts, B., Edwin, P.M., Benz, A.O. On coronal oscillations. Astrophys. J. 279, 857–865, 1984.

Sakurai, T., Ichimoto, K., Raju, K.P., et al. Spectroscopic observation of coronal waves. Sol. Phys. 209, 265–286, 2002.

Uchida, Y. Diagnosis of coronal magnetic structure by flare-associated hydromagnetic disturbances. Pub. Astron. Soc. Jap 22, 341, 1970.

Van Doorsselaere, T., Debosscher, A., Andries, J., et al. The effect of curvature on quasi-modes in coronal loops. Astron. Astrophys. 424, 1065–1074, 2004.

Verwichte, E., Foullon, C., Nakariakov, V.M. Fast magnetoacoustic waves in curved coronal loops. Astron. Astrophys. 446, 1139–1149, 2006.

Verwichte, E., Nakariakov, V.M., Ofman, L., et al. Characteristics of transverse oscillations in a coronal loop arcade. Sol. Phys. 223, 77–94, 2004.

Wang, T.J., Solanki, S.K., Curdt, W., et al. Hot coronal loop oscillations observed with SUMER: examples and statistics. Astron. Astrophys. 406, 1105–1121, 2003.

Wang, T., Solanki, S.K., Curdt, W., Innes, D.E., et al. Doppler shift oscillations of hot solar coronal plasma seen by SUMER: a signature of loop oscillations? Astrophys. J. 574, L101–L104, 2002.

Williams, D.R. Diagnosing MHD wave detections in solar coronal loops: torsional effects. ESA SP-547: SOHO 13 Waves, Oscillations and Small-Scale Transients Events in the Solar Atmosphere: Joint View from SOHO and TRACE 13, 513–518, 2004.

Zaitsev, V.V., Stepanov, A.V. On the origin of the hard X-ray pulsations during solar flares. Sov. Astron. Let. 8, 132–134, 1982.

Zaitsev, V.V., Stepanov, A.V. On the origin of pulsations of type IV solar radio emission . Plasma cylinder oscillations (I). Issled. Geomagn. Aeron. Fiz. Solntsa 37, 3–10, 1975.

Zaitsev, V.V., Kislyakov, A.G., Stepanov, A.V., et al. Pulsating microwave emission from the star AD Leo. Astron. Let. 30, 319–324, 2004.

Zaqarashvili, T.V. Observation of coronal loop torsional oscillation. Astron. Astrophys. 399, L15–L18, 2003.

Zhugzhda, Y.D., Nakariakov, V.M. Linear and nonlinear magnetohydrodynamic waves in twisted magnetic flux tubes. Phys. Let. A 252, 222–232, 1999.